Pressure Dependence of the Oxidation State of Manganese and Magnetic Property of CaLaMgMnO$_{6-x}$

Jin-Ho Choy*, Seung-Tae Hong, Nam-Gyu Park, Song-Ho Byeon[†], and Gérard Demazeau[‡]

Department of Chemistry, College of Natural Sciences, Seoul National University, Seoul 151-742, Korea
[†]*Department of Chemistry, College of Natural Sciences, Kyung Hee University, Kyungki 449-701, Korea*
[‡]*Laboratoire de Chimie du Solide du CNRS, Université Bordeaux I, 33405 Talence, Cedex, France*
Received September 8, 1994

Oxygen deficient perovskites CaLaMgMnO$_{6-x}$ were prepared in three different oxygen pressures; at 1150 C under oxygen gas pressure of 0.1 MPa (*L*), at 950 ℃ under 0.1 GPa (*M*), and at 900 ℃ under high pressure of 6 GPa (*H*). From iodometric titration and EPR spectra, the samples could be formulated as (CaLa)(MgMn^{II},Mn^{III},Mn$^{IV}_{1-y}$,$_y$)O$_{5.43}$ (2*x*−*y*=0.14) (*L*), CaLaMgMn$^{III}_{0.1}$Mn$^{IV}_{0.9}$O$_{5.43}$ (*M*) and CaLaMgMn$^{IV}_{0.93}$Mn$^{VI}_{0.07}$O$_{5.57}$ (*H*), and it could be confirmed that Mn (IV) ions are the most stable in an octahedral site of perovskites, but a small content of Mn(II), Mn(III) or Mn(VI) ions are also stabilized in an oxygen-vacant site due to the site preferences of such ions, depending on the oxygen pressure. The anomalous magnetic properties of *L* and *M* might result from the simultaneous occurrence of antiferromagnetism and ferromagnetism below T_C or T_N, which could be explained by semicovalence magnetic exchange model.

Introduction

The unusual high oxidation states of transition metal ions in various oxide lattices are generated by controlling the three main factors; (a) the structurla factors, namely, size and symmetry of the cation site; (b) the nature of the cationic surroundings, that is, the covalent bonding character and the influence of competing bonds, and (c) the high oxygen pressures. It has been found that the 4d and 5d elements, such as Nb, Mo, Ru, Ta, Re, Os and Ir with high oxidation state (V) could be stabilized in a perovskite lattice more easily compared to 3d elements thanks to their lower ionization potentials.[1~5] Therefore the tetravalent and pentavalent 3d ions stabilized in an O$_h$ symmetry are not so well known except for La$_2$LiMO$_6$ oxides, where *M* = vanadium[6,7] manganese[8], or iron.[9~11] The Mn(V) ion is also an unusual oxidation state and due to its size and d^2 electronic configuration, its normal coordination is tetrahedral. Only one example of Mn (V) stabilized in an oxide with the perovskite structure has ever been described recently by us.[8] Therefore, we have tried to extend our study for stabilizing the Mn(V) in the other perovskite lattice with the general formula ALaMgMnO$_6$ (*A* = Ca, Sr, Ba) using high oxygen pressure of 6 GPa. But, the oxygen deficient perovskites ALaMgMnO$_{6-x}$(0<*x*<0.5; *A* = Ca, Sr, Ba) with the mixed valence state of manganese have been produced reproducibly.[12~14]

In the perovskite type AA′BB′O$_6$ or A$_2$BB′O$_6$ oxides, the O-2*p* orbitals participate in π-bonding with B′ cation, and σ-bonding with A, A′ cation. Thus π(B′-O) and σ(A-O) bonds are competing each other, and the strength of σ(B′-O) is correlated to σ(B-O) bonds. Therefore the covalency of the (B′-O) bonds is influenced by the nature of both A and B cations. From this view point it can be deduced that if B cation is the same, then the (B′-O) covalency would be governed only by the nature of A-site cation.[15]

In order to stabilize a high oxidation state of Mn(V) in such a perovskite lattice, high covalency in the (Mn-O) bond should be derived.; The competing σ(B′-O) bond must be as weak as possible and also the perpendicularly competing bond should be less covalent. The perovskite type with A(II) A′(III)B(II)B′(V)O$_6$ was selected to investigate the alkaline earth metal (A) substitution effect, where La(III) was selected as A′ cation which is the largest cation with +III charge, and Mg ion was chosen as B cation which is the smallest alkaline earth metal ion except Be. In the present study, in order to underline the pressure effect on the stabilization of manganese ions in perovskites we have prepared and characterized the same material with the formula of CaLaMgMnO$_{6-x}$ under the different preparation conditions (0.1 MPa (*L*), 0.1 GPa (*M*) oxygen pressure, and 6 GPa (*H*) using belt-type apparatus.

Experimental

CaLaMgMnO$_{6-x}$ were prepared from high purity CaCO$_3$, La$_2$O$_3$, Mg(NO$_3$)$_2$6H$_2$O and MnO$_2$. Equimolar mixtures were homogeneously ground in an agate mortar, pelleted and calcined at 700 ℃ in order to decompose the carbonates and nitrates. The samples were reground and repelleted and sintered at 850 ℃ for 12 hours. *L* was finally sintered at 1150 ℃ for 10 hrs under oxygen flowing atomosphere of 0.1 MPa (1 bar),[16] and *M* was again fired at 950 ℃ for 12 hours and finally treated under the high oxygen gas pressure of 0.1 GPa (1 kbar) at 950 ℃ for 48 hours.[17] *H* was obtained by treating at 900 ℃ for 15 minutes under 6 GPa (60 kbar) using a belt-type high pressure apparatus.[12] Oxygen was generated *in situ* by thermal decomposition of KClO$_3$[2KClO$_3$ →2KCl+3O$_2$(g)], which was intermixed with the sample in the high pressure cell, for achieving the high oxidation state of manganese. The remaining KCl in the material was removed by washing with distilled H$_2$O and absolute ethanol.

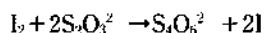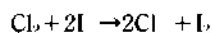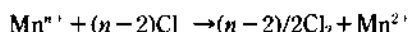After the reactions were completed, the resultant phases were identified by powder X-ray diffraction method with a

Table 1. Pressure Dependencies of Unit Cell Parameters, Average Oxidation State of Manganese and Chemical Formula for CaLaMg-MnO$_6$ ₓ

Pressure given during preparation	0.1 MPa	0.1 GPa	6 GPa
Unit cell parameters[a]	$a = 3.847$ Å	$a = 3.864$ Å	$a = 3.823$ Å
Average oxidation state of Mn[b]	3.86	3.90	4.14
Oxygen vacancy (X)	0.57	0.55	0.43
Chemical formula	CaLaMgMnO$_{5.43}$	CaLaMgMnO$_{5.45}$	CaLaMgMnO$_{5.57}$

[a]Mg and Mn ions are disordered; [b]According to redox titration.

Philips-Norelco diffractometer using Ni filtered Cu-Kα radiation ($\lambda = 1.5418$ Å). The oxidation state of manganese was determined by indirect iodometric method. After dissolution of the sample in a KI solution, the evolved free iodine was titrated by sodium thiosulfate. These procedures are summarized as follows:

$$Mn^{n+} + (n-2)Cl \rightarrow (n-2)/2Cl_2 + Mn^{2+}$$

$$Cl_2 + 2I \rightarrow 2Cl + I_2$$

$$I_2 + 2S_2O_3^{2-} \rightarrow S_4O_6^{2-} + 2I$$

($n \geq 2$: average oxidation state of manganese ion)

The magnetic susceptibility has been measured by Faraday-type magnetobalance in the temperature range of 4.2 K and 300 K and the EPR spectrum could be obtained at 4.2 K and room temperature using Bruker-ER 200 tt X-band spectrometer.

Results and Discussion

Crystallographic Analysis. The powder X-ray diffraction patterns indicate that the perovskites *L*, *M*, and *H* have simple cubic unit cells with $a = 3.847$ Å, 3.864 Å and 3.823 Å respectively, indicating the disordered arrangement of Mg and Mn cations in the octahedral site of the perovskites. According to Galasso *et al.*,[18] the differences in the valence and the size between B and B' cations are the important factors for inducing an 1/1 order in such perovskite-type compounds. Considering that the difference in the charge is close to 2 (a large part of Mn ions are as Mn(IV) and that the difference of ionic radii of Mg and Mn ions are not so small (the ionic radii of Mg(II) and Mn(IV) being 0.72 and 0.53 Å respectively), the disordering might be attributed to the mixed valence state of manganese ion and to the formation of oxygen vacancies, which would reduce the possible Madelung ordering energy.

Chemical Analysis. In order to form an ideal stoichiometric perovskite CaLaMgMnO$_6$, all the manganese ion in the lattice must be pentavalent Mn(V) by the charge neutrality condition. However, the average valence state of manganese was estimated to be 3.86 (*L*), 3.90 (*M*) and 4.14 (*H*) according to the iodometric titration as shown in Table 1, indicating the existence of oxygen deficiency and also implying that a large part of manganese ions are stabilized as Mn(IV), and a few of them as Mn(III), Mn(II) or higher valences. For this reason such perovskites can be formulated as CaLaMgMnO$_{5.43}$ (*L*), CaLaMgMnO$_{5.45}$ (*M*) and CaLaMgMnO$_{5.57}$ (*H*), respectively.

EPR Spectroscopic Study. EPR and magnetic suscep-
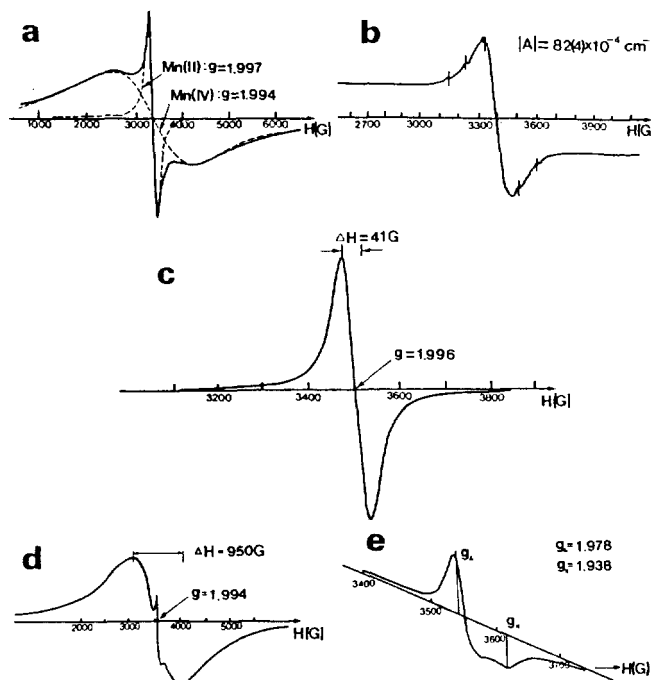
Figure 1. Pressure dependencies of EPR spectra for CaLaMg-MnO$_{6-x}$ (*L*) at room temperature. (a) *L* (0.1 MPa), (b) *L*; the enlarged spectrum of the signal in (a), (c) *M* (0.1 GPa), (d) *H* (6 GPa), and (e) *H*; the enlarged spectrum of weak signal in (d).

tibility measurements have been carried out to confirm the oxidation state of the manganese ions. The EPR spectra for *L* at room temperature indicate the existence of two kinds of paramagnetic species in the perovskite lattice (Figure 1 (a)), which shows that the observed signal is a superposition of two isotropic components of a broad isotropic signal ($\Delta H = 1600$ G, $g = 1.994 \pm 0.002$) with one sharp signal ($\Delta H \cong 50$ G, $g = 1.997 \pm 0.002$). They might correspond respectively to Mn(II) and Mn(IV) ions. Figure 1(b) is an enlarged spectrum of the sharp signal appeared in a resonance range of 2700-4100 cm^{-1} of Figure 1(a). Here we could observe the hyperfine structure clearly. The observed g-values of 1.997(2) and hyperfine coupling constant of 82×10^{-4}cm^{-1} is very close to those of Mn(II) in LiNbO$_2$ ($g = 1.998(1)$, $|A| = 78 \times 10^{-4}$ cm^{-1}),[19] and Mn(II) in ZnMoO$_4$ ($g = 1.994(1)$, $|A| = 82(4) \times 10^{-4}$ cm^{-1}).[20] The observed g-value of 1.994(2) from the broad signal is rather very close to those of Mn(IV) in La$_2$Li-MnO$_{6-x}$ ($g = 1.999$),[8] Mn(IV) in SrLa$_3$LiMnO$_8$ ($g = 1.995$),[21] Mn (IV) in SrTiO$_3$ ($g = 1.994$),[22,23] Mn(IV) in α-Al$_2$O$_3$ ($g = 1.994$),[24]

Pressure Dependence of the Oxidation State of Mn

Bull. Korean Chem. Soc. **1995** *Vol. 16, No. 2* 107

Table 2. Pressure Dependencies of g-values of Manganese in $CaLaMgMnO_6$.

Pressure	g (300 K)	Remarks
$CaLaMgMnO_{5.43}$	1.997(2)	$|A| = 82(4)^a$: Mn(II)
(0.1 MPa)	1.994(2)	Mn(IV) in O_h site
$CaLaMgMnO_{5.43}$	1.996	Weak ferromagnetic
(0.1 GPa)		coupling
		at lower temperature
$CaLaMgMnO_{5.57}$	$g_\perp = 1.978$,	Mn(VI) in T_d site
(6 GPa)	$g_t = 1.938$	Mn(IV) in O_h site
	$g = 1.994$	
$CaLaMgMnO_{5.5}{}^b$	1.996	Mn(IV) in O_h site

^{a} $|A|$ denotes the absolute value of the hyperfine coupling constant with unit of 10^{-4} cm^{-1}. ^{b} The thermal decomposition products of high pressure (6 GPa) treated samples (^{b}) after thermogravimetric analysis up to around 350 $^\circ$C.

and Mn(IV) in $CaZrO_3$ $(g = 1.994)$.[25] Though any signal corresponding to Mn(III) was not observed at 300 K and even at 4.2 K due to its very short spin-lattice relaxation time, an existence of a small Mn(III) fraction in the lattice should be taken into account, which will be discussed in magnetic section in detail along with the experimental confirmation. Therefore we can formulate L as $(CaLa)(MgMn^{II}{}_x Mn^{III}{}_y Mn^{IV}{}_{1-x-y})O_{5.43}$ $(2x + y = 0.14)$.

The EPR spectrum for M at room temperature shows a sharp isotropic signal with $g = 1.996$ and $\Delta H \cong 41$ G (Figure 1(c)). The observed g-value corresponds exactly to that from Mn(IV) in various oxides.[8,21~25] There is no additional signal which might be attributed to Mn(II), Mn(V), or Mn(VI) ions. Thus M can be formulated as $CaLaMgMn^{III}{}_{0.1}Mn^{IV}{}_{0.9}O_{5.45}$.

According to the EPR spectra at room temperature for (H), it is believed to be two kinds of paramagnetic species in the lattice due to the super-imposition of a wide and narrow signals (Figure 1(d) and 1(e)). The wide intense signal with $g = 1.994$ is attributed to the Mn(IV) in octahedral coordination. A sharp weak resonance at $g_\perp \approx 1.978$ and $g_\parallel = 1.938$ from the enlarged spectrum (Figure 1(e)) is attributable to the Mn(VI) $(3d^1)$ not in octahedral coordination but in pseudo-tetrahedral site, which was disappeared upon heating. This interpretation is most probable due to the anisotropic nature of the EPR signal. The EPR spectrum of Mn(VI) in K_2CrO_4 at 20 K shows an anisotropic signal $(g_x = 1.970 \pm 0.005, g_y = 1.966 \pm 0.001, g_z = 1.938 \pm 0.001,$[26] which is quite consistent with our observation. If the weak signal could have been attributed to Mn(V) $(3d^2)$ in an octahedral environment, an EPR signal should have been observed below 4 K. On the other hand Mn(V) in a tetrahedral site can be easily detected by EPR at room temperature but with a higher g value $(g = 2.02 \pm 0.01)$.[27] Therefore the above assumptions on the paramagnetic Mn(V) in an octahedral or a tetrahedral coordination should be excluded. The experimental results of redox titration $(Mn^{4.14})$ and EPR measurements suggest the existence of Mn(IV) and Mn(VI) only, therefore, the composition of the high-pressure sample could be formulated as $CaLaMgMn^{IV}{}_{0.93}Mn^{VI}{}_{0.07}O_{5.57}$.

Effect of Covalency and Distribution of Oxygen Vacancy. The structural distortion, symmetry preference

of transition metal ions and abnormal magnetic properties in various oxides with spinel and perovskite-type structures were explained excellently by the theory of semicovalence proposed by Goodenough.[28] As will be shown later, the semicovalent model is quite appropriate for predicting the distribution of oxygen vacancy as well as explaining the magnetic property of $CaLaMgMnO_6$ $_x$. In such a model, it is pointed out that because of the strong perturbations of neighboring atoms on one another, the empty energy levels correspond to lattice orbitals, not atomic orbitals, and these lattice orbitals may have energies which are nearly degenerated with the atomic d orbitals. The most stable hybrid lattice orbitals for various valence state of manganese ions are d^2sp^3 (octahedral) for Mn(IV) (d^3), dsp^2 (square planar) for Mn(III) (d^4), sp^3 for Mn(II) (d^5) or Mn(VI) (d^1).[28,29] If the most stable of the empty cation orbitals strongly overlap the full orbitals of neighboring anions, the anion p electrons may spend some of their time in the cation orbitals. The full anion p orbital contains two electrons of opposite spin. If the cation has an oriented net moment, these electrons will not have an equal probability of being shared by the cation. Because of the presence of exchange forces, that anion electron whose spin is parallel to the net cation spin will spend more time on the cation than that with antiparallel spin. Because a single electron predominates in this bond, it is called semicovalent. Another postulate for semicovalence is that it occurs only below Curie or Neel temperature where the net cation magnetic moment is oriented. Above T_C or T_N there is normal coordinate covalence.
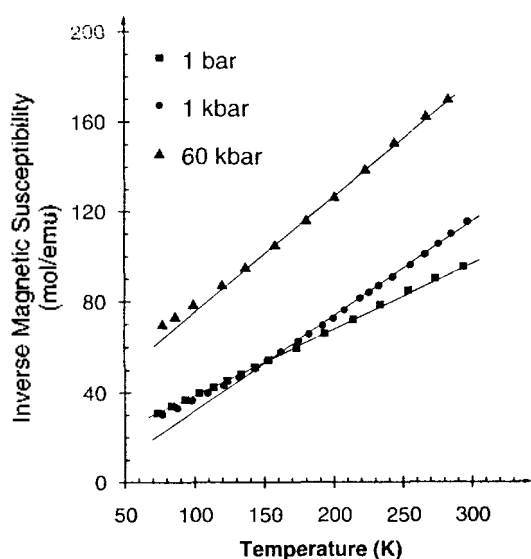
Now let us consider the distribution of oxygen vacancies. Because the total content of Mn(III) and/or Mn(II) or Mn(VI) in L, M and H is so small (about 14%, 10%, and 7%, respectively), it can be reasonably assumed that they must be diluted in the lattice. In addition Mn and Mg ions are distributed randomly in the octahedral site of the perovskite. Therefore, there are three possible Mn-O bonding types in L, two Mn-O ones in M and H as listed in Table 3. The dotted line represents a quite ionic bonding character.

Based upon the postulate of formation of stable hybrid orbitals, it is easily deduced that Mn(IV) ions prefer the 6-coordinated octahedral site and Mn(III) ions favor the oxygen vacant site having square planar symmetry. On the other hand, Mn(II) and Mn(VI) ions have little symmetry preference because they might form a less covalent bond in these perovskites. Of course, the sp^3 orbitals may form a covalent bond with its four neighboring oxygen ions. An octahedral site with oxygen cis-vacancies can be transformed into a tetrahedral one through a slight displacement of manganese ion.[12] However, in this case, the formation of $Mn(sp^3)$-$O(p)$ covalent bond on one side of an oxygen ion may weaken the orbital overlap between the $Mn^{IV}(d^2sp^3)$-$O(p)$ covalent bond on the opposite side of the anion, for the Mn(II or VI)-O-Mn(IV) bond is no longer linear. Therefore it is concluded that Mn(II)-O and Mn(VI)-O bonds may be less covalent in L and H perovskites, and the ions would have various local symmetries caused by oxygen vacancies. The relative energies for various symmetries around the Mn(II) or Mn (VI) ion would not greatly differ in magnitude due to the depression of covalency.

The broad EPR signals (Figure 1(a) and 1(d)) for Mn(IV) ion in samples of L and H supports the existence of strong

Table 3. Pressure Dependencies of the Nature of the Chemical Bonding between Manganese and Oxygen Ions, and Possible Magnetic Interactions between Manganese Ions, and Effective Magnetic Moments in $CaLaMgMnO_{6-x}$

	0.1 MPa	0.1 GPa	6 GPa
Chemical formula	$CaLaMgMn^{II}_xMn^{III}_y$ $Mn^{IV}_1{}_{-x}O_{5.43}(2x+y=0.14)$	$CaLaMgMn^{III}_{0.1}Mn^{IV}_{0.9}O_{5.43}$	$CaLaMgMn^{V}_{0.93}Mn^{VI}_{0.07}O_{5.57}$
Possible Mn-O bondings	$Mn^{IV}(d^2sp^3)$-$O(2p)$ $Mn^{III}(dsp^2)$-$O(2p)$ $Mn^{II}(sp^3)\cdots O(2p)$	$Mn^{IV}(d^2sp^3)$-$O(2p)$ $Mn^{III}(dsp^2)$-$O(2p)$	$Mn^{IV}(d^2sp^3)$-$O(2p)$ $Mn^{VI}(sp^3)\cdots O(2p)$
Possible magnetic interactions between Mn ions	Mn(IV)-O-Mn(IV) antiferromag. Mn(IV)-O-Mn(III) antiferromag. Mn(IV)-O$\cdots$Mn(III) weak ferromag. Mn(IV)-O$\cdots$Mn(II) weak ferromag. Mn(IV)-O$\cdots$Mn(III)+ Mn(III)$\cdots$O-Mn(IV) ferromag.	Mn(IV)-O-Mn(IV) antiferromag. Mn(IV)-O-Mn(III) antiferromag. Mn(IV)-O$\cdots$Mn(III) weak ferromag. Mn(IV)-O$\cdots$Mn(III)+ Mn(III)$\cdots$O-Mn(IV) ferromag.	Mn(IV)-O-Mn(IV) antiferromag. Mn(IV)-O$\cdots$Mn(VI) weak ferromag.
Effective magnetic moment	5.23	4.31	3.8

Figure 2. Reciprocal molar susceptibility for $CaLaMgMnO_{6-x}$ prepared under 0.1 MPa (*L*), 0.1 GPa (*M*) and 6 GPa (*H*).

covalency in Mn(IV)-O bond, and the sharp signal for Mn(II) ion may result from the ionic (less covalent) character of Mn(II)-O and Mn(VI)-O bonds. And the doublet-like signals of hyperfine structure for Mn(II) ion might be caused by the presence of different local symmetries of the ions due to the oxygen vacancy. For sample *M*, it is also most probable that Mn(III) ions favor the oxygen vacant site having square planar symmetry, which result in only one signal due to Mn(IV) ion in EPR spectrum (Figure 1(c)).

Magnetic Property. In Figure 2, the temperature dependencies of inverse molar magnetic susceptibilities for *L*, *M* and *H* are shown. Diamagnetic contribution of every ion is corrected according to Selwood.[30] They follow the Curie-

Weiss law between 20 K and 300 K (*L*), between 200 K and 400 K (*M*) and between 80 K and 600 K (*H*), with Curie constants of $C=3.42$ (*L*), 2.32 (*M*) and 2.07 (*H*) with the effective magnetic moment of $\mu_{eff}=2.828\sqrt{C}=5.23$ B.M. (*L*), 4.31 B.M. (*M*) and 4.07 B.M. (*H*), and Weiss constant of $\theta=34$ K (*L*), 29 K (*M*) and -66 K (*H*), respectively. The *C* and θ were obtained from the least square fit of $\chi_m^{-1}=(T-\theta)/C$ in the temperature domain following the Curie-Weiss law.

Now let us consider the magnetic behavior of *L*, first. Generally the orbital motions of 3*d* electrons in crystal lattice are quite quenched by ligand ions.[31] Thus, in the absence of magnetic interaction between 3*d* metal ions, the observed moments are well consistent with the spin-only values. Therefore, the spin-only value of the effective magnetic moment for $(CaLa)(MgMn^{II}_xMn^{III}_yMn^{IV}_{1-x-y})O_{5.43}$ $(2x+y=0.14)$ can be calculated as 4.04 ± 0.01 B.M.; Consider two extreme cases, where $x=0$ and $y=0$.

(1) $x=0$ or $y=0.14$.
  $(\mu_{eff,1})^2=0.14\times\mu_{eff}^2(Mn^{III})+0.86\times\mu_{eff}^2(Mn^{IV})=16.3$, or
  $\mu_{eff,1}=4.03$ B.M.
(2) $y=0$ or $x=0.07$
  $(\mu_{eff,2})^2=0.07\times\mu_{eff}^2(Mn^{II})+0.93\times\mu_{eff}^2(Mn^{IV})=16.4$, or
  $\mu_{eff,2}=4.05$ B.M.

Then it should be noted that the observed moment of 5.23 B.M. is quite larger than the spin-only value, implying the existence of magnetic coupling at lower temperature between manganese ions through the shared oxygen ions in the perovskite lattice. The negative Weiss constant (-34 K) calculated from the data set above 20 K implies an antiferromagnetic interaction at low temperature domain. However, the large magnetic moment 5.23 B.M. and relatively large magnetic susceptibilities could not be understood by considering pure antiferromagnetism only. Thus it has been proposed that the anomalous magnetism may be due to small ferromagnetic domain in the lattice, and the semicovalent model can be

used to explain the simultaneous occurrence of antiferro- and ferromagnetism in the sample. Here it is necessary to point out that above T_C or T_N, most of magnetic materials show paramagnetism obeying the Curie-Weiss law. However, the ferro- or antiferromagnetic properties below T_C or T_N are still reflected even in this paramagnetic temperature region.; *i.e.* the ferro- and the antiferromagnetic materials still have relatively large and small magnetic susceptibilities above T_C and T_N, respectively, compared to the coupling free susceptibilities.

There might be three kinds of manganese pairs which may produce magnetic interactions in the lattice of the perovskite : Mn(IV)-O-Mn(IV), Mn(IV)-O-Mn(III), and Mn(IV)-O-Mn(II) (see Table 3). Because of the small content of Mn(II) and Mn(III) (about 14%), it can be assumed reasonably that the interactions between Mn(II) and Mn(III) can be neglected. Then major magnetic interactions in this lattice should be originated from Mn(IV)-O-Mn(IV) interaction.

Four mechanisms, known as direct exchange, double exchange, superexchange, and semicovalent exchange have been used to explain the interaction between electron spins. The direct exchange tends to align the net spin on neighboring lattice elements antiparallel to each other. Double exchange requires the transfer of electrons between two kinds of ions, particularly two of the same elements but with different charges. It tends to align spins parallel to each other. Superexchange predicts that the two cations orient their spin parallel if their *d*-shell are less than half filled, antiparallel if the *d*-shells are more than half filled. The semicovalent exchange model is based upon the postulate for semicovalence described previously. According to this model, there are five possible magnetic couplings between manganese ions in $CaLaMgMnO_{6-x}$ as represented in Table 3. This exchange model predicts that if an anion *p* orbital forms semicovalent bond with two neighboring cations on opposite side of the anion, an antiferromagnetic coupling may result in, and if semicovalence occurs with one cation only, the interaction between the anion and other cations is confined to direct exchange, and consequently a weak ferromagnetic coupling may occur. If both two neighboring Mn(IV) and Mn(III) ions are stabilized in octahedral symmetry and covalence occurs only in Mn(IV)-O bond, then the state Mn(IV)-O ··· Mn(III) is degenerated with the state Mn(III) ··· O-Mn(IV), so that below T_C double exchange takes place between the manganese ions, namely, one electron being free to jump through the anion between the two manganese ions to form a metallic-like bond.[28] As can be seen in Table 3, the semicovalent exchange model predicts that there must be simultaneous occurrence of antiferromagnetism and ferromagnetism in L [(CaLa)(MgMn$^{II}_x$Mn$^{III}_y$Mn$^{IV}_{1-x-y}$)O$_{5.43}$ $(2x+y=0.14)$]. Of course the antiferromagnetic coupling must be a major interaction due to the large content of Mn(IV)-O-Mn(IV) interaction. In the superexchange model there is no way for atoms to couple ferromagnetically in one direction, antiferromagnetically in another as it contains no anisotropy. From superexchange model, L should be ferromagnetic. This is not consistent with the observed magnetic data. Therefore, based upon the semicovalent magnetic exchange model, the anomalous magnetic property of L in its paramagnetic temperature region might result from the simultaneous occurrence of antiferromagnetism and ferromagnetism below T_C or T_N.

As in the case of L, the effective magnetic moment of M [CaLaMgMn$^{III}_{0.1}$Mn$^{IV}_{0.9}$O$_{5.45}$] can be calculated as : $\mu_n^2 = 0.1 \times \mu_n^2(Mn^{III}) + 0.90 \times \mu_n^2(Mn^{IV}) = 0.1 \times (4.90)^2 + 0.90 \times (3.87)^2 = 15.9$ or $\mu_n = 4.0$ B.M. Then the observed moment of 4.31 is somewhat larger than the spin-only value, implying the existence of magnetic coupling between manganese ions. There might be also two kinds of possible magnetic interactions in the lattice : Mn(III)-O-Mn(IV) and Mn(IV)-O-Mn(IV) (Table 3). And assuming the semicovalence, it is most probable that the manganese ions are ferromagnetically coupled in the latter case. Therefore the somewhat larger value of observed magnetic moment might result from the possible ferromagnetic interaction between Mn(III) and Mn(IV) ions in M; which is also consistent with the positive value of the observed Weiss constant. But the antiferromagnetic coupling [Mn(IV)-O-Mn(IV)] at low temperatures could not be excluded completely, because of the small positive curvature, indicating the antiferromagnetic transition, in the χ_m^{-1} *vs.* T plot (Figure 2) below 200 K.

In the case of H (CaLaMgMnO$_{5.77}$), the possible magnetic interactions are Mn(IV)-O-Mn(IV) and Mn(IV)-O-Mn(VI). Since the Mn(VI) would, however, prefer a tetrahedrally coordinated site, the strength of magnetic interaction between Mn(IV)-O-Mn(VI) would be significantly diminished due to the tilting angle of Mn(IV)-O-Mn(VI) bond. Thus the interaction between the Mn(VI) ions will be predominant in H, which resulted in the magnetic behavior with the effective magnetic moment of 4.07 B.M. consistent with spin-only value (3.87 B.M.) of Mn(IV).

References

1. Nakamura, T.; Choy, J. H. *J. Solid State Chem.* **1977**, *20*, 233.
2. Choy, J. H.; Kim, D. K.; Demazeau, G.; Jung, D. Y. *J. Phys. Chem.* **1994**, *98*, 6258.
3. Hayashi, K.; Demazeau, G.; Pouchard, M.; Hagenmuller, P. *Mater. Res. Bull.* **1980**, *15*, 461.
4. Hayashi, K.; Demazeau, G.; Pouchard, M. *C.R. Acad. Sci.* Série II, **1981**, *292*, 1433.
5. (a) Choy, J. H.; Hong, S. T.; Kang, S. G. *Proc. Int'l Symp. Fine Ceramics, Arita '89*, **1989**, Yamaguchi Insatsu, Arita, p 69. (b) Choy, J. H. *New Ceramics*, **1991**, *4*, 87.
6. Choy, J. H.; Byeon, S. H.; Demazeau, G. *J. Solid State Chem.* **1988**, *76*, 97.
7. Demazeau, G.; Kim, E. O.; Choy. J. H.; Hagenmuller, P. *Mater. Res. Bull.* **1987**, *22*, 735.
8. Demazeau, G.; Kim, E. O.; Choy. J. H.; Hagenmuller, P. *J. Solid State Chem.* **1992**, *101*, 221.
9. Demazeau, G.; Buffat, B.; Ménil, F.; Fournes, L.; Pouchard, M.; Dance, J. M.; Fabritchnyi, P.; Hagenmuller, P. *Mater. Res. Bull.* **1981**, *16*, 1465.
10. Choy, J. H.; Demazeau, G.; Byeon, S. H. *Solid State Commun.* **1991**, *77*(9), 647.
11. Choy, J. H.; Demazeau, G.; Byeon, S. H. *Solid State Commun.* **1991**, *80*(9), 683.
12. Choy, J. H.; Demazeau, G.; Dance, J. M. *J. Solid State Chem.* **1990**, *84*, 1.

13. Choy, J. H.; Demazeau, G.; Byeon, S. H.; Dance, J. M. *J. Phys. Chem. Solids* **1990**, *51*, 391.
14. Choy, J. H.; Demazeau, G.; Hong, S. T. *Jpn. J. Appl. Phys.* **1992**, *31*, 3649.
15. Goodenough, J. B. *Phys. Rev.* **1967**, *164*(2), 785.
16. Choy, J. H.; Hong, S. T.; Kim, S. J. *J. Korean Ceram. Soc.* **1991**, *28*(8), 603.
17. Choy, J. H.; Hong, S. T. *Bull. Korean Chem. Soc.* **1991**, *12*(3), 349.
18. Galasso, F. S.; Katz, L.; Ward, R. *J. Am. Chem. Soc.* **1959**, *81*, 820.
19. Takeda, T.; Watanabe, A.; Sugihara, K. *Phys. Lett.* **1968**, *A27*, 114.
20. Dernov-Pigarev, V. F.; Zaripov, M. M.; Samoiloich, M. I.; Stepanov, V. G. *Fiz. Tverd. Tela.* **1965**, *7*, 3688.
21. Kim, E.; Demazeau, G.; Dance, J. M.; Pouchard, M.; Hagenmuller, P. *C.R. Acad. Sci.* Ser. 2, **1985**, *16*, 491.

22. Müller, K. A. *Helv. Phys. Acta.* **1960**, *33*, 497.
23. Müller, K. A. *Phys. Rev. Lett.* **1959**, *2*, 341.
24. Geschwind, S.; Kisliuk, R.; Klein, M. P.; Remeika, J. P.; Wood, D. L. *Phys. Rev.* **1962**, *126*, 1684.
25. Henderson, B. *Proc. Phys. Soc.* **1967**, *92*, 1064.
26. Carrington, A.; Ingram, D. J. E.; Lott, K. A. K. *Proc. Roy. Soc. London*, **1960**, *A254*, 101.
27. Luwig, G. W.; Woodbury, H. H. *Solid State Physics*; Vol. 1, eds. Seitz, F. and Turnbull, D.; Academic Press: New York, 1962.
28. Goodenough, J. B. *Phys. Rev.* **1955**, *100*, 564.
29. Goodenough, J. B.; Loeb, A. L. *Phys. Rev.* **1955**, *98*(2), 391.
30. Selwood, P. W. *Magnetochemistry*; 2nd ed.; chap. 5; Interscience: New York, 1967.
31. Figgis, B. N. *Introduction to Ligand Fields*; Interscience: New York, 1966.

Modified LOGIT(MLOGIT) Transformation: Prediction of IC$_{50}$ Value from Two Arbitrary Concentration Data

Sung-Eun Yoo* and Ok Ja Cha

Korea Research Institute of Chemical Technology, Daedeog-Danji, Taejon 305-606, Korea
Received September 9, 1994

A LOGIT transformation is a method to estimate IC$_{50}$ values with two arbitrary concentration data when complete dose response curves (DRCs) are not available. We propose a modified LOGIT transformation (MLOGIT) which predicts IC$_{50}$ values more accurately than the conventional LOGIT method.

Introduction

In a QSAR (Quantitative Structure Activity Relationship) analysis, a thermodynamic property representing biological responses is commonly expressed in IC$_{50}$ value which is the molar concentration of a compound resulting in a half-maximum inhibition response. The IC$_{50}$ is normally obtained experimentally from dose response curves. However, it is troublesome to obtain complete dose response curves due to several practical reasons.

Therefore, a logit transformation[1,2] has been developed as a way of predicting IC$_{50}$ when only two arbitrary concentration data are available. A logit transformation is carried out as follows:[2]

1. The logit transformed formula at the concentrations C is: $\log [R_c/(100-R_c)]$

R_c = Response in % at the concentration C

2. $L_c = \log [R_c/(100-R_c)] - \log C$

L_c = logit value at the concentration C

3. $\text{LOGIT} = (L_{c1} + L_{c2})/2$

L_{c1} and L_{c2} are logit values at concentrations $C1$ and $C2$.

This transformation is based on the assumption that all compounds would have the same shape of dose response curves and that the response would be within the linear part of the sigmoidal dose response curve. Also it is based on the assumption that one response is less than 50% and the other one is more than 50%.

Table 1. LOGIT and MLOGIT value[a]

#	C1	R_{c1}	C2	R_{c2}	L_{c1}	L_{c2}	LOGIT	MLOGIT
1	3	29	10	64	5.13	5.25	5.19	5.20
2	3	29	32	88	5.13	5.36	5.25	5.21
3	10	64	32	88	5.25	5.36	5.31	5.19

[a]$C1$ and $C2$ are concentration in μm of compound 6 in reference 3. R_{c1} and R_{c2} are response in % at concentration $C1$ and $C2$. L_{c1} and L_{c2} are logit value at concentration $C1$ and $C2$. Observed pI_{50} of compound 6 is 5.20.

Results and Discussion

The LOGIT values calculated using data from Table 1 in reference 3 are plotted against the observed pI_{50}, log(1/IC$_{50}$), to show a good correlation ($r^2 = 0.994$) in Figure 1.[4]

However, as shown in Figure 1, the LOGIT values vary depending on the response values used. For example, if